

control of fine metal particles. Moreover, this method has many advantages with respect to the experimental conditions, because a parallel laser beam is used for irradiation.

It is also noteworthy that isomerization among *cis*-2-butene, *trans*-2-butene, and 1-butene via *cis*-*trans* isomerization and 1,3-hydrogen transfer processes has been observed in a mixture of SF<sub>6</sub>-Fe(CO)<sub>5</sub>-butene irradiated by a TEA CO<sub>2</sub> laser light.<sup>36</sup> In the isomerization reactions the coordinatively unsaturated iron carbonyls act as catalytic species. The generation of a catalytic species from transition metal carbonyls via the SF<sub>6</sub>-photosensitized

decomposition will be one of the candidates for application of a TEA CO<sub>2</sub> laser to organic syntheses.

**Acknowledgment.** Thanks are due to Satoru Utsuno, Mitsuhiro Kurokawa, Shigeru Ishikawa, and Tatsuki Kawamura, undergraduate students of Science University of Tokyo in 1984-1988, for their collaboration in the course of the experiments. We are grateful to Yasuhiro Iimura for X-ray diffractometry, and Dr. Tesshu Miyahara and Ryugo Maeda in Dainippon Ink & Chemicals for TEM photographs.

## Design of Redox Systems for the Selective Transport of Electrons across Liquid Membranes: Nickel(II,III) Tetraaza Macrocyclic Complexes

Giancarlo De Santis, Michela Di Casa, Mario Mariani, Barbara Seghi, and Luigi Fabbrizzi\*

Contribution from the Dipartimento di Chimica Generale, Università di Pavia, 27100 Pavia, Italy. Received February 22, 1988

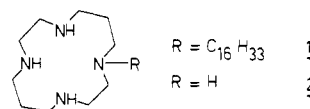
**Abstract:** The complexes NiLX<sub>2</sub> (L = *N*-cetylcyclam; X = Cl, ClO<sub>4</sub>) have been synthesized to be used as carriers for the transport of electrons across a CH<sub>2</sub>Cl<sub>2</sub> bulk liquid membrane, through the Ni<sup>II</sup>/Ni<sup>III</sup> redox change. Two-phase (water/dichloromethane) experiments have shown that aqueous peroxydisulfate ion is able to oxidize Ni<sup>II</sup>LCl<sub>2</sub>, but not Ni<sup>II</sup>L(ClO<sub>4</sub>)<sub>2</sub>, due to the very large difference of the Ni<sup>III,II</sup> redox potentials. On the other hand, the [Ni<sup>III</sup>LCl<sub>2</sub>]Cl complex in the organic layer can be reduced by a series of aqueous cationic reducing agents, according to a rate sequence (Ti<sup>III</sup> > Cr<sup>II</sup> > Fe<sup>II</sup> > [Co<sup>II</sup> cage] complex) that does not correlate with their redox potential values. The anionic reducing agent I<sup>-</sup> does not reduce [Ni<sup>III</sup>LCl<sub>2</sub>]Cl under two-phase conditions, whereas it does in homogeneous conditions. Three-phase experiments have not been performed in which electrons are transported from an aqueous reducing phase, containing the metal-centered agents mentioned above, to an aqueous oxidizing phase, containing peroxydisulfate and chloride, across a CH<sub>2</sub>Cl<sub>2</sub> membrane containing the [Ni<sup>II</sup>LCl<sub>2</sub>]/[Ni<sup>III</sup>LCl<sub>2</sub>]Cl redox couple. A counterflow of Cl<sup>-</sup> anions is coupled to the flow of electrons. Under the conditions employed, the electron transport is complete in a time ranging from minutes (reducing agent, Ti<sup>III</sup>) to several hours ([Co<sup>II</sup> cage] complex).

A liquid membrane is a water-immiscible organic layer (bulk or supported on a microporous film) that separates two aqueous layers. Experiments on the transport of chemical entities across bulk or supported liquid membranes have been designed by many researchers in the past decade, with the aim being to mimic and rationalize biological processes and also because of important practical applications. Much of the work has been devoted to the transport of metal ions,<sup>1</sup> mainly of the s block, and involved the design of appropriate carriers able to complex in a selective way the cation in the liquid membrane. On the other hand, in spite of the fundamental role of redox active membranes in biology, very few studies have been reported on the transport of electrons across liquid membranes. The above studies have considered as electron carriers classical metal complexes, like ferrocene<sup>2</sup> and nickel bisdithiolene,<sup>3</sup> or organic substrates, like quinones,<sup>2,4,5</sup> whereas charge neutrality in the membrane was ensured through the simultaneous flow of anions, cations, or protons. In these studies attention has been centered on the design of the electron-transport experiment, to be coupled to a flow of cations or to a counterflow of anions, and on the control of the transport

by a concentration gradient (eventually photochemically generated).<sup>2,5</sup>

In the present work we were interested in designing a redox system, to be used as an electron carrier, whose redox potential could be controlled, in order to perform the *selective* transport of electrons from an electron source phase (ESP) to an electron receiving phase (ERP). In a selective transport, the carrier should be able to discriminate among a mixture of reducing agents in ESP and/or a mixture of oxidizing agents in ERP.

As a potentially modulable electron carrier, we have used a system based on the Ni<sup>II</sup> and Ni<sup>III</sup> complexes of the novel tetraaza macrocycle *N*-cetylcyclam (**1**, L). It is well documented that



encircling of nickel(II) by the precursor tetraaza macrocycle cyclam (**2**) permits easy attainment, in solution of polar solvents (H<sub>2</sub>O, MeCN, DMSO), of the otherwise unstable trivalent state whose chemistry has been extensively investigated in the past years.<sup>6</sup> Appending a C<sub>16</sub> aliphatic chain on the cyclam framework makes the nickel(II,III) complexes soluble in apolar and poorly polar solvents, immiscible with water, to be used as a liquid membrane. Since these solvents have no coordinating ability, the

(1) Izatt, S. R.; Hawkins, R. T.; Christensen, J. J.; Izatt, R. M. *J. Am. Chem. Soc.* **1985**, *107*, 63-68. Di Casa, M.; Fabbrizzi, L.; Perotti, A.; Poggi, A.; Riscassi, R. *Inorg. Chem.* **1986**, *25*, 3984-3987, and references therein.

(2) Grimaldi, J. J.; Boileau, S.; Lehn, J. M. *Nature (London)* **1977**, *265*, 229-330.

(3) Grimaldi, J. J.; Lehn, J. M. *J. Am. Chem. Soc.* **1979**, *101*, 1333-1334.

(4) Danesi, P. R. *J. Membr. Sci.* **1986**, *29*, 287-293.

(5) Jackman, D. C.; Thomas, C. A.; Rillema, D. P.; Callahan, R. W.; Yan, S.-L. *J. Membr. Sci.* **1987**, *30*, 213-225.

(6) Fabbrizzi, L. *Comments Inorg. Chem.* **1985**, *4*, 33-54, and references therein.

metal complexes exist in the membrane as  $[\text{Ni}^{\text{II}}\text{LX}_2]$  and  $[\text{Ni}^{\text{III}}\text{LX}_2]\text{X}$  intact species, in which the  $\text{X}^-$  anion, through ligand field effects, may alter the relative stability of  $[\text{Ni}^{\text{II}}\text{LX}_2]$  and  $[\text{Ni}^{\text{III}}\text{LX}_2]\text{X}$  species, thus making the  $\text{Ni}^{\text{III/II}}$  redox potential change and controlling the oxidation and reduction processes that occur at the membrane interfaces with aqueous ERP and ESP.

We describe in this work the transport of electrons across a bulk  $\text{CH}_2\text{Cl}_2$  membrane, which contains as a carrier a  $\text{Ni}(\text{N-cetyl-cyclam})\text{X}_2$  complex. Preliminary two-phase oxidation and reduction experiments have shown that the ligating ability of the anion  $\text{X}^-$  (the strongly coordinating chloride ion, or the weakly coordinating perchlorate ion) dramatically affects the course of the redox changes at the interface, allowing or not allowing the electron transfer through a bulk  $\text{CH}_2\text{Cl}_2$  membrane to occur.

### Experimental Section

**Synthesis of *N*-Cetyl cyclam (1, L).** An ethanolic solution of cetyl bromide,  $\text{C}_{16}\text{H}_{33}\text{Br}$  (6.5 mmol in 20  $\text{cm}^3$ ), was added dropwise to a stirred solution of cyclam (32.5 mmol) in ethanol/acetonitrile (100/300  $\text{cm}^3$ ) at room temperature. The solution was refluxed for 12 h and then rotovaporated to dryness. The white residue was extracted five times with aqueous  $\text{NaOH}$ /ether (50/50  $\text{cm}^3$ ). The ethereal extract, dried overnight over anhydrous sodium sulfate, was evaporated to give a white waxy precipitate of **1**: yield 2.51 g (91%). Anal. Calcd for  $\text{C}_{26}\text{H}_{56}\text{N}_4$ : C, 73.52; H, 13.29; N, 13.19. Found: C, 73.01; H, 13.30; N, 12.90.

**Synthesis of  $\text{NiCl}_2$  and  $\text{Ni}(\text{ClO}_4)_2 \cdot 6\text{H}_2\text{O}$  ( $\text{X} = \text{Cl}, \text{ClO}_4$ )** was dissolved in butanol and partly evaporated to eliminate most of the water. The hot butanolic solution of the nickel salt was added dropwise to a stirred boiling butanolic solution of **1** (solutions of both metal salt and ligand were  $10^{-2}$  M). A precipitate of the metal complex formed, violet for  $\text{NiCl}_2$  and yellow for  $\text{Ni}(\text{ClO}_4)_2$ , which was recrystallized from  $\text{CH}_2\text{Cl}_2/\text{C}_2\text{H}_5\text{OH}$ : yield  $\text{NiCl}_2$  49%,  $\text{Ni}(\text{ClO}_4)_2$  56%. Anal. Calcd for  $\text{NiC}_{26}\text{H}_{56}\text{N}_4\text{Cl}_2$ : C, 56.33; H, 10.18; N, 10.11. Found: C, 56.08; H, 10.55; N, 9.89. Anal. Calcd for  $\text{NiC}_{26}\text{H}_{56}\text{N}_4\text{O}_8\text{Cl}_2$ : C, 45.77; H, 8.27; N, 8.21. Found: C, 46.00; H, 8.55; N, 7.99.

**Electrochemistry.**  $E_{1/2}$  values for the  $\text{Ni}^{\text{III}}\text{LX}_3/\text{Ni}^{\text{II}}\text{LX}_2$  redox change were determined through voltammetric studies using a conventional three-electrode cell in which the working electrode was a platinum microsphere, the counter electrode was a platinum foil, and the reference electrode was a silver wire. The deaerated  $\text{CH}_2\text{Cl}_2$  solution, 0.1 M in  $\text{Bu}_4\text{NX}$  (C. Erba, Milan, polarographic grade), was made  $10^{-3}$  M both in the  $\text{NiLX}_2$  complex and in ferrocene (to calibrate, as an internal standard, the pseudoreference silver electrode). The electrochemical apparatus employed has already been described.<sup>7</sup>

**Two-Phase Redox Processes.** Oxidation processes in two-phase conditions were performed by placing in a test tube, equipped with a stopper, 7  $\text{cm}^3$  of  $\text{CH}_2\text{Cl}_2$   $10^{-3}$  M in  $\text{NiLX}_2$  and an equal volume of an aqueous solution 0.1 M in  $\text{Na}_2\text{S}_2\text{O}_8$  and 1 M in  $\text{NaX}$ . The closed test tube was vigorously shaken for 60 s by an oscillating electromechanical stirrer (Bicasa, Milan). Formation of the trivalent nickel complex (bright yellow) was demonstrated by the appearance of the typical absorption band in the UV region ( $\nu = 324$  nm,  $\epsilon = 8150$   $\text{dm}^3 \text{mol}^{-1} \text{cm}^{-1}$ ). Further shaking did not increase the intensity of the band.

To evaluate the effect of the concentration of the reagents (e.g., aqueous  $\text{Cl}^-$ ) on the rate of the oxidation process, a layer of dichloromethane containing  $[\text{Ni}^{\text{II}}\text{LCl}_2]$  (7  $\text{cm}^3$ ) and an aqueous layer containing  $\text{Na}_2\text{S}_2\text{O}_8$  (0.1 M) and  $\text{NaCl}$  (7  $\text{cm}^3$ ) were stratified in a cylindrical vessel of radius 2.0 cm. The  $\text{CH}_2\text{Cl}_2$  layer was magnetically stirred at 200 rpm. Formation of the  $[\text{Ni}^{\text{III}}\text{LCl}_2]\text{Cl}$  species was monitored through the intensity of the band at 324 nm; in particular, 0.25- $\text{cm}^3$  portions of the organic layer were carefully extracted with a syringe at selected time intervals and placed in a 1-mm quartz cuvette, and their spectra were measured on a Cary 2300 UV-VIS-NIR spectrophotometer. The  $\text{CH}_2\text{Cl}_2$  portion was then returned by syringe to the layer in the vessel.

For two-phase reduction experiments, the  $[\text{Ni}^{\text{III}}\text{LCl}_2]\text{Cl}$  complex in the  $\text{CH}_2\text{Cl}_2$  layer was generated through oxidation by aqueous peroxydisulfate (vide supra). The aqueous oxidizing layer was carefully removed with a syringe; the nonaqueous layer was washed three times with equal volumes of aqueous 1 M  $\text{NaCl}$ . Then, the reducing aqueous layer was added and the two phases were vigorously mixed. Occurrence of the reduction of the  $\text{Ni}^{\text{III}}\text{LX}_3$  complex in  $\text{CH}_2\text{Cl}_2$  was observed through the disappearance of the nickel(III) complex UV band.

Kinetic studies of the reduction processes were carried out by the same procedure as described for oxidation processes (vide supra). In this case special care was taken to avoid oxygen contamination of the aqueous and

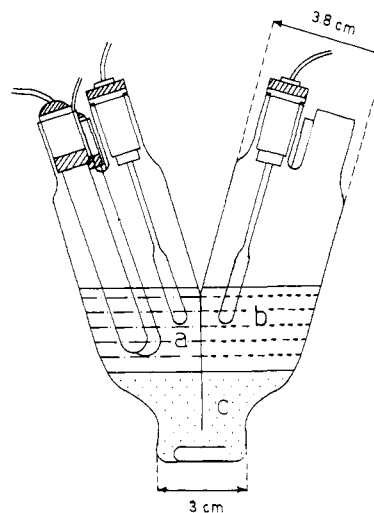


**Figure 1.** Glass vessel used in electron transport experiments: (a) aqueous layer (e.g., electron source phase, ESP, typically 25  $\text{cm}^3$ ); (b) aqueous layer (e.g., electron receiving phase, ERP, 25  $\text{cm}^3$ ); (c) membrane ( $\text{CH}_2\text{Cl}_2$ , 25  $\text{cm}^3$ ). The membrane is magnetically stirred; ESP and ERP are stirred by rotating glass rods, driven by twin electric motors, at a constant speed. Two electrodes (indicator and reference) can be dipped in ESP to monitor the progress of an electron transport experiment, through the potential of the aqueous  $\text{M}^{(\text{n}+1)+}/\text{M}^{\text{n}+}$  redox couple.

organic layers. Disappearance of the  $[\text{Ni}^{\text{III}}\text{LCl}_2]\text{Cl}$  species was followed spectrophotometrically. Reducing aqueous solutions ( $10^{-2}$  M in the reducing agent) were prepared by dissolving the appropriate salt ( $\text{NaI}$ ,  $(\text{NH}_4)_2\text{Fe}(\text{SO}_4)_2 \cdot 12\text{H}_2\text{O}$ ) under anaerobic conditions in deaerated aqueous solution 1 M in  $\text{Cl}^-$  ( $\text{NaCl}$  for  $\text{I}^-$  and  $\text{HCl}$  for  $\text{Fe}^{\text{II}}$ ). Aqueous  $\text{Cr}^{\text{II}}$  was prepared through reduction of a  $\text{CrCl}_3$  solution, 1 M in  $\text{HCl}$ , by zinc amalgam.<sup>8</sup> Zinc amalgam was also used to prepare aqueous  $[\text{Co}^{\text{II}}(\text{diamsarH}_2)]^{4+}$ , through reduction of a solution of the  $[\text{Co}^{\text{III}}(\text{diamsarH}_2)]\text{Cl}_5$  complex, 1 M in  $\text{HCl}$ . The  $\text{Ti}^{\text{III}}$  solution was prepared by dilution with hydrochloric acid of a commercially available standard solution of  $\text{TiCl}_3$  (C. Erba, Milan).

**Electron Transport Experiments.** For transport experiments the V-shaped glass cell sketched in Figure 1 was used. In this vessel the two aqueous layers (ESP and ERP, 25  $\text{cm}^3$  each) were separated by a  $\text{CH}_2\text{Cl}_2$  layer of 25  $\text{cm}^3$  (the liquid membrane) and by a glass wall. The membrane,  $10^{-3}$  M in the carrier, was magnetically stirred at 200 rpm. The two aqueous layers were mechanically stirred by two glass rods driven by two twin electric motors, at a constant rate (200 rpm). The arms of the V-shaped cell could be fitted with electrodes (indicating and reference). In particular, the progress of the electron transport could be monitored through the potential difference between a mercury electrode and a calomel electrode, dipped in the ESP compartment. During the transport experiments, nitrogen saturated in  $\text{CH}_2\text{Cl}_2$  flowed in both arms of the cell.

### Results and Discussion

**Design of the Redox System.** When encircled by a cyclic polyamine, the  $\text{Ni}^{\text{II}}$  cation can be easily oxidized, chemically or anodically, to the authentic trivalent ( $d^7$ , low-spin) complex.<sup>11</sup> Detailed electrochemical investigations on the oxidation behavior in acetonitrile solution of  $\text{Ni}^{\text{II}}$  complexes with a complete series of quadri-, quinque-, and sexidentate macrocycles of varying atomicity<sup>12</sup> have shown that the easiest formation of the  $\text{Ni}^{\text{III}}$  species, expressed by the least positive value of the  $\text{Ni}^{\text{III/II}}$  electrode potential, occurs with the symmetric 14-membered quadridentate macrocycle cyclam (**2**). This property results from the ability of cyclam to exert the strongest in-plane metal-nitrogen interactions,

(8) Bassett, J.; Jeffery, G. H.; Mendham, J. *Vogel's Textbook of Quantitative Inorganic Analysis*, 4th ed.; Longman: London, 1978; p 397.

(9) Diamsar, 1,8-diamino-3,6,10,13,16,19-hexaazabicyclo[6.6.6]heptacosane.  $[\text{Co}^{\text{III}}(\text{diAmsarH}_2)]\text{Cl}_5$  was prepared as described by Sargeson et al.<sup>10</sup>

(10) Geue, R. J.; Hambley, T. W.; Harrowfield, J. M.; Sargeson, A. M.; Snow, M. R. *J. Am. Chem. Soc.* **1984**, *106*, 5478-5488.

(11) LoVecchio, F. V.; Gore, E. S.; Busch, D. H. *J. Am. Chem. Soc.* **1974**, *96*, 3109-3118.

(12) Bencini, A.; Fabbrizzi, L.; Poggi, A. *Inorg. Chem.* **1981**, *20*, 2544-2549. Buttafava, A.; Fabbrizzi, L.; Perotti, A.; Poggi, A.; Poli, G.; Seghi, B. *Inorg. Chem.* **1986**, *25*, 1456-1460.

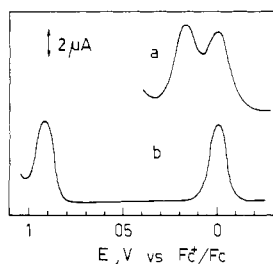
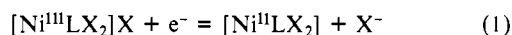


**Figure 2.** Alternating current voltammetry profiles in  $\text{CH}_2\text{Cl}_2$  solution, at  $25^\circ\text{C}$ : (a)  $10^{-3}$  M in  $\text{Ni}(\text{N-cetyl cyclam})\text{Cl}_2$  and in ferrocene, 0.1 M in  $\text{Bu}_4\text{NCl}$ ; (b)  $10^{-3}$  M in  $\text{Ni}(\text{N-cetyl cyclam})(\text{ClO}_4)_2$  and in ferrocene, 0.1 M in  $\text{Bu}_4\text{NClO}_4$ . The less anodic peak in each profile refers to the  $\text{Fc}/\text{Fc}^+$  internal reference couple.

which raise the energy of the antibonding orbital, essentially metallic in character, from which the electron is abstracted in the oxidation process. Moreover, metal complexes of cyclam, both in the divalent and trivalent states, are especially resistant toward demetalation, even under very drastic conditions.<sup>13</sup> Thus, we have chosen to use as an electron carrier a system based on cyclam, in particular its  $\text{Ni}^{\text{II}}$  and  $\text{Ni}^{\text{III}}$  complexes. In order to satisfy the typical requirements of carrier systems for membrane experiments (1. solubility in the membrane, e.g.,  $\text{CH}_2\text{Cl}_2$ ; 2. complete insolubility in water), a  $\text{C}_{16}$  aliphatic chain has been appended to the cyclam framework through a nitrogen atom. Synthesis of *N*-cetyl cyclam (**1**, **L**) involved the nucleophilic substitution of cetyl bromide on one of the four equivalent secondary amine groups of the cyclam precursor. Synthesis is very conveniently carried out through reaction of cetyl bromide with a 5-fold excess of cyclam (to minimize the formation of polysubstituted derivatives). Separation of the desired product **1** from unreacted cyclam is made especially easy by the very different solubility properties of cyclam and *N*-cetyl cyclam (extraction with aqueous  $\text{NaOH}$ /ether).

$\text{Ni}^{\text{II}}\text{LX}_2$  complexes have been isolated as pure solids through reaction of **L** with a slight excess of the hydrated  $\text{NiX}_2$  salt in butanolic solution:  $\text{X} = \text{Cl}$ , violet, high-spin;  $\text{X} = \text{ClO}_4$ , yellow, low-spin. The anions were chosen in view of (i) their very different coordinating tendencies (as clearly reflected by the spin state of the  $\text{Ni}^{\text{II}}$  metal center) and (ii) their limited or nil reducing properties, which should exclude any interference in the oxidation processes at the aqueous-phase/membrane interface (*vide infra*).

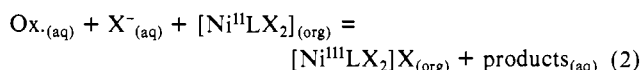
The  $\text{Ni}^{\text{III}}/\text{Ni}^{\text{II}}$  redox change for the cetyl cyclam complexes has been characterized electrochemically, by performing voltammetric investigations on  $\text{CH}_2\text{Cl}_2$  solutions made  $10^{-3}$  M in  $\text{NiLX}_2$  and 0.1 M in  $\text{Bu}_4\text{NX}$  ( $\text{X} = \text{Cl}, \text{ClO}_4$ ), using a platinum microsphere as working electrode. One-electron reversible profiles were obtained (see Figure 2), whose half-wave potential values, measured versus the ferrocenium/ferrocene internal reference, are as follows:  $E_{1/2}([\text{Ni}^{\text{III}}\text{LX}_2]/[\text{Ni}^{\text{II}}\text{LX}_2]) = 0.175$  V;  $E_{1/2}([\text{Ni}^{\text{III}}\text{L}(\text{ClO}_4)_2]/[\text{Ni}^{\text{II}}\text{L}(\text{ClO}_4)_2]) = 0.920$  V. Notice how marked is the effect of the anion  $\text{X}^-$  on the  $\text{Ni}^{\text{III}}/\text{Ni}^{\text{II}}$  redox potential (750 mV difference between the chloride and perchlorate complex), even larger than that observed in the case of MeCN solutions of polyaza macrocyclic complexes, where apical donors remained constant (acetonitrile molecules) and the denticity and the atomicity of the macrocycle were varied.<sup>12</sup> The redox change in  $\text{CH}_2\text{Cl}_2$  is to be ascribed to the following half-reaction:



Both the trivalent and divalent species present in reaction 1 exhibit a more or less distorted octahedral stereochemistry in which the axial sites are occupied by the  $\text{X}^-$  anions.<sup>14</sup> The  $\text{Ni}^{\text{II}}-\text{ClO}_4$

axial interaction is so weak as to permit the stabilization of the singlet state.  $E_{1/2}(\text{Ni}^{\text{III}}/\text{Ni}^{\text{II}})$  values indicate that the very coordinating chloride ion strongly favors the access to the trivalent state, compared to the weakly coordinating perchlorate ion. This behavior reflects the capability of a tripositive cation (e.g.,  $\text{Ni}^{\text{III}}$ ) to profit from the ligand field to a larger extent than a dipositive one (e.g.,  $\text{Ni}^{\text{II}}$ ).

**Two-Phase Redox Processes: Oxidation of  $[\text{Ni}^{\text{II}}\text{LX}_2]$ .** In order to assess the appropriate conditions for the electron transport (three-phase) experiments, two-phase oxidation and reduction processes were preliminarily investigated in their thermodynamic and kinetic aspects. First, the oxidation of the  $[\text{Ni}^{\text{II}}\text{LX}_2]$  complex in the organic phase by an aqueous oxidizing agent was considered. The process is described by following equation:



The very strong aqueous oxidizing agent peroxydisulfate ( $E^0 = 1.96$  V vs NHE) was used in the oxidation tests described by eq 2. A  $7\text{-cm}^3$  aliquot of an aqueous solution 0.1 M in  $\text{Na}_2\text{S}_2\text{O}_8$  and 1 M in  $\text{NaX}$  was vigorously shaken in a stoppered test tube with  $7\text{ cm}^3$  of a  $\text{CH}_2\text{Cl}_2$  solution  $10^{-3}$  M in  $[\text{Ni}^{\text{II}}\text{LX}_2]$ . When  $\text{X} = \text{Cl}$ , the violet organic solution of the divalent complex turned bright yellow ( $\nu = 324$  nm,  $\epsilon = 8150$  dm<sup>3</sup> mol<sup>-1</sup> cm<sup>-1</sup>), due to the formation of the trivalent complex.  $\text{S}_2\text{O}_8^{2-}$  is known to react slowly in homogeneous conditions in the absence of an appropriate catalyst.<sup>15</sup> However, the presently investigated two-phase reaction appears to be extremely fast, and the simple stratifying of the aqueous peroxydisulfate layer over the organic layer, even in the absence of any stirring, makes the yellow color of the  $\text{Ni}^{\text{III}}$  complex immediately appear at the interface and diffuse into the dichloromethane solution. However, when  $\text{X} = \text{ClO}_4$ , even after prolonged shaking, the  $\text{Ni}^{\text{III}}$  absorption band does not develop at all in the organic layer, i.e., the two-phase oxidation of the  $\text{Ni}^{\text{II}}\text{L}(\text{ClO}_4)_2$  complex does not take place. The above results indicate that aqueous  $\text{S}_2\text{O}_8^{2-}$ , as an oxidizing agent, is not strong enough to oxidize the  $\text{Ni}^{\text{II}}\text{L}(\text{ClO}_4)_2$  complex. Thus, trying to juxtapose the electrochemical series in water (vs NHE) and in dichloromethane (vs the  $\text{Fc}^+/\text{Fc}$  reference couple), the  $E^0([\text{Ni}^{\text{III}}\text{LCl}_2]/[\text{Ni}^{\text{II}}\text{LCl}_2])$  value should lie below the aqueous  $\text{S}_2\text{O}_8^{2-}/\text{SO}_4^{2-}$  redox couple potential, whereas the  $E^0([\text{Ni}^{\text{III}}\text{L}(\text{ClO}_4)_2]/[\text{Ni}^{\text{II}}\text{L}(\text{ClO}_4)_2])$  value should lie above.<sup>16</sup> Other strong aqueous oxidizing agents, e.g.,  $\text{Ce}^{\text{IV}}$  in perchloric acid solution ( $E^0 = 1.70$  V vs NHE), do not oxidize the lipophilic  $\text{Ni}^{\text{II}}\text{L}(\text{ClO}_4)_2$  complex in two-phase conditions. The same agents could not be employed in two-phase experiments where  $\text{X} = \text{Cl}$ , since chlorine developed. Thus, formation of the trivalent species could be more likely ascribed to the single-phase oxidation by  $\text{Cl}_2$  dissolved in the  $\text{CH}_2\text{Cl}_2$  layer, rather than to a two-phase redox change.

In any case, at this stage of the work, it appears that the two-phase reduction of aqueous oxidizing agent  $\text{S}_2\text{O}_8^{2-}$  by the  $\text{Ni}^{\text{II}}\text{LX}_2$  complex can be thermodynamically controlled by varying the nature of  $\text{X}^-$ , i.e., its coordinating tendencies toward the metal center of the nonaqueous system.

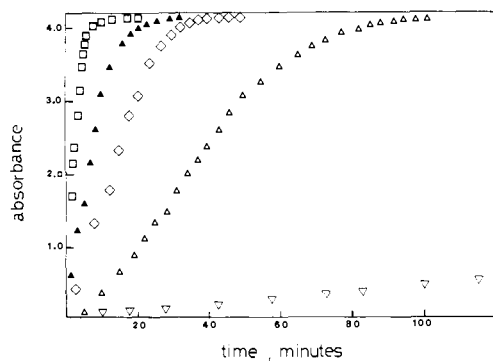
(15) Bard, A. J.; Parsons, R.; Jordan, J. *Standard Potentials in Aqueous Solution*; Marcel Dekker: New York, 1985; p 107.

(16) In the present circumstances, the use of the potential values determined through voltammetric experiments is not correct. In fact, electrochemically determined potential values refer to a  $\text{CH}_2\text{Cl}_2$  solution 0.1 M in  $\text{Bu}_4\text{NX}$ . On the contrary, in the two-phase experiments no  $\text{Bu}_4\text{NX}$  has been added to the  $\text{CH}_2\text{Cl}_2$  layer. As suggested by a reviewer, the  $[\text{X}^-]$  concentration in a  $\text{CH}_2\text{Cl}_2$  solution equilibrated with an aqueous solution 1 M in  $\text{NaX}$  can be calculated by using the partition coefficient values reported by Abraham and Liszi:<sup>17</sup>  $\log K(\text{water}/\text{dichloromethane}) \text{Cl}^- = -8.7$ ;  $\text{ClO}_4^- = -1.8$ . Thus, substituting these values in the Nernst equation, actual potential values for the  $[\text{Ni}^{\text{III}}\text{LX}_2]/[\text{Ni}^{\text{II}}\text{LX}_2]$  redox change become for  $\text{X} = \text{Cl}$ , 0.69 V and  $\text{X} = \text{ClO}_4$ , 1.03 V vs  $\text{Fc}^+/\text{Fc}$ . Therefore, the two electrochemical scales in water and dichloromethane should be juxtaposed in such a way that the aqueous peroxydisulfate potential lies between the corrected values of nickel chloride and perchlorate complexes reported above. In any case, use of measured or corrected potential values does not alter the sense of the discussion.

(17) Abraham, M. H.; Liszi, J. *J. Inorg. Nucl. Chem.* **1981**, *43*, 143.

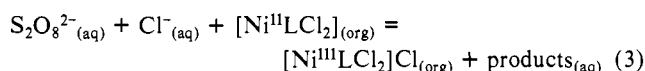
(13) Busch, D. H. *Acc. Chem. Res.* **1978**, *11*, 392-400.

(14) Bulk generation of the  $[\text{Ni}^{\text{III}}\text{LCl}_2]\text{Cl}$  complex in  $\text{CH}_2\text{Cl}_2$  was performed by bubbling dichlorine in a dichloromethane solution of  $[\text{Ni}^{\text{II}}\text{LCl}_2]$ . The ESR spectrum of the solution frozen at 77 K displayed axial symmetry with the  $g_{\perp}$  value considerably greater than  $g_{\parallel}$  (2.18 and 2.03, respectively). Moreover, the  $g_{\parallel}$  feature was split into seven lines ( $A_{\parallel} = 27$  G). The above evidence is consistent with the formation of an authentic  $\text{Ni}^{\text{III}}$  ( $d^7$ , low-spin) complex, having an elongated octahedral stereochemistry, and in which the apical positions are occupied by two equivalent chloride ions ( $I_{\text{Cl}} = 3/2$ ).



**Figure 3.** Plot of the absorbance of the band at 324 nm of the  $[\text{Ni}^{\text{III}}\text{LCl}_2]\text{Cl}$  complex in  $\text{CH}_2\text{Cl}_2$  vs time during two-phase oxidation by aqueous  $\text{S}_2\text{O}_8^{2-}$ . Rate-depressing effect of the aqueous chloride concentration:  $\text{CH}_2\text{Cl}_2$  layer,  $5 \times 10^{-4}$  M in  $[\text{Ni}^{\text{III}}\text{LCl}_2]$ ; aqueous layer, 0.1 M in  $\text{Na}_2\text{S}_2\text{O}_8$ . Varying concentration of NaCl:  $\square$ , 0.1 M;  $\blacktriangle$ , 0.3 M;  $\diamond$ , 0.5 M;  $\triangle$ , 1.0 M;  $\nabla$ , 2.0 M.

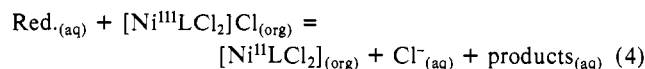
Kinetic aspects of the two-phase oxidation process have been considered through time-dependent studies of reaction 3. In



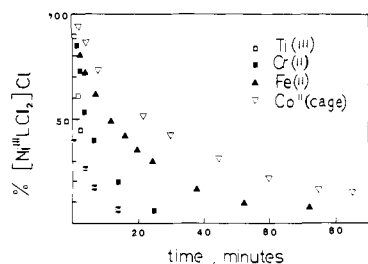
particular, the formation of the  $[\text{Ni}^{\text{III}}\text{LCl}_2]\text{Cl}$  complex has been followed through the increase of the intense band of the trivalent chromophore at 324 nm, in experiments in which a  $\text{CH}_2\text{Cl}_2$  layer was magnetically stirred at a constant rate, under an aqueous layer of equal volume containing  $\text{Na}_2\text{S}_2\text{O}_8$  and NaCl. In particular, we wished to consider the effect of the concentration of aqueous chloride ion, which appears as a reactant in eq 3, on the rate of the two-phase redox process. Thus, in a series of experiments, the concentrations of aqueous  $\text{S}_2\text{O}_8^{2-}$  and of the  $[\text{Ni}^{\text{III}}\text{LCl}_2]$  complex in the  $\text{CH}_2\text{Cl}_2$  layer were kept constant (0.1 and  $5 \times 10^{-4}$  M, respectively), whereas the concentration of NaCl in the aqueous layer was varied.

Figure 3 describes the increase with time of the absorbance of the  $\text{Ni}^{\text{III}}$  band (at 324 nm) in two-phase experiments in which the chloride concentration in the aqueous layer ranged from 0.1 to 2.0 M. Figure 3 shows that the rate of the two-phase oxidation process drastically decreases with the increasing concentration of aqueous chloride. In particular, we have observed that at a NaCl concentration greater than 3 M the oxidation of the  $\text{Ni}^{\text{III}}$  complex does not take place at all. This result is in full contrast with what one could expect on the basis of the two-phase process described by eq 3 and should probably be related to the modification exerted by  $\text{Cl}^-$  ions of the structure of the solution in the vicinity of the interface. It is possible that the increasing concentration of chloride ions in the bulk solution, as well as in the layer where the electron transfer takes place, makes more and more difficult, through crowding or electrostatic repulsion effects, the approach of the anionic oxidizing agent to the reducing metal center.<sup>18</sup> However, whatever the intimate mechanism of the chloride effect is, a new element of selectivity has been introduced that could allow modulation of the rate of the two-phase oxidation of the redox system to be used as an electron carrier.

**Two-Phase Redox Processes: Reduction of  $[\text{Ni}^{\text{III}}\text{LX}_2]\text{X}$ .** In a similar way, the two-phase reduction of the nonaqueous oxidized metal complex has been investigated; the process can be described by the following equation:



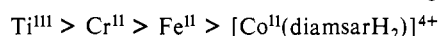
(18) In an other series of experiments, the concentration of aqueous chloride was varied and the ionic strength of the aqueous phase was adjusted to 1 M with  $\text{NaClO}_4$ . However, increase of the perchlorate concentration was found to stop the two-phase oxidation: this is to be ascribed to the  $\text{ClO}_4^-/\text{Cl}^-$  exchange in the two-phase system and to the replacement of chloride by perchlorate in the axial sites of the  $\text{Ni}^{\text{III}}$  complex, which raises the  $\text{Ni}^{\text{III}}/\text{Ni}^{\text{II}}$  potential and prevents the oxidation by  $\text{S}_2\text{O}_8^{2-}$ .



**Figure 4.** Plot of the percent of the  $[\text{Ni}^{\text{III}}\text{LCl}_2]\text{Cl}$  complex in the  $\text{CH}_2\text{Cl}_2$  layer vs time during two-phase reduction experiments by aqueous reducing agents:  $\square$ ,  $\text{Ti}^{\text{III}}$ ;  $\blacktriangle$ ,  $\text{Cr}^{\text{II}}$ ;  $\blacktriangle$ ,  $\text{Fe}^{\text{II}}$ ;  $\nabla$ ,  $[\text{Co}^{\text{II}}(\text{diamsarH}_2)]^{4+}$ . Aqueous layer, 0.10 M in the reducing agent, 1.0 M in HCl;  $\text{CH}_2\text{Cl}_2$  layer,  $10^{-3}$  M in  $[\text{Ni}^{\text{III}}\text{LCl}_2]\text{Cl}$ .

Preliminarily, a  $\text{CH}_2\text{Cl}_2$  solution of the  $[\text{Ni}^{\text{III}}\text{LCl}_2]\text{Cl}$  complex has been equilibrated with an equal volume of an aqueous acidic solution containing a one-electron cationic reducing agent:  $\text{Fe}^{\text{II}}$ ,  $\text{Ti}^{\text{III}}$ ,  $\text{Cr}^{\text{II}}$ , and  $[\text{Co}^{\text{II}}(\text{diamsarH}_2)]^{4+}$ . In each case, reduction of the nonaqueous trivalent complex takes place, as indicated by the disappearance of the intense yellow color in the organic layer.

Kinetic aspects of the above two-phase redox processes have been investigated in conditions of controlled magnetic stirring of the  $\text{CH}_2\text{Cl}_2$  layer, as described in the previous paragraph. The aqueous reducing agent was 200 times more concentrated than the nonaqueous oxidized metal complex (0.10 and 0.0005 M, respectively). Moreover, the aqueous layer was made 1 M in HCl, in order to maintain the same chloride concentration as in corresponding two-phase oxidation experiments and to prevent the hydrolysis of the metal ion. Progress of the reaction was followed by recording the absorption spectra of the  $\text{CH}_2\text{Cl}_2$  layer at chosen time intervals and monitoring the decrease of the band at 324 nm. Figure 4 describes the variation of the concentration of the  $[\text{Ni}^{\text{III}}\text{LCl}_2]\text{Cl}$  complex (in percentage, calculated from the ratio of the absorbance at 324 nm vs its limiting value) for experiments with metal-centered reducing agents. Figure 4 shows that the two-phase reduction of the nonaqueous  $\text{Ni}^{\text{III}}$  complex is extremely fast with  $\text{Ti}^{\text{III}}$  and becomes slower and slower along the series



Noticeably, the above series does not correlate with the sequence of the standard electrode potentials:  $\text{Fe}^{\text{III}}/\text{Fe}^{\text{II}} = 0.77$  V vs NHE;  $\text{Ti}^{\text{IV}}/\text{Ti}^{\text{III}} = 0.09$ ;  $[\text{Co}^{\text{III}}(\text{diamsarH}_2)]^{5+}/[\text{Co}^{\text{II}}(\text{diamsarH}_2)]^{4+} = 0.05$ ;  $\text{Cr}^{\text{III}}/\text{Cr}^{\text{II}} = -0.43$ .

It should be considered that the above metal ions, under the experimental conditions employed, exist as chloro complexes or aqua-chloro complexes. Thus, it may be possible that the electron transfer from the aqueous reducing agent to the nonaqueous oxidized complex occurs at the water/dichloromethane interface via a chloride ion bridging the  $\text{Ni}^{\text{III}}$  and the M center ( $\text{M} = \text{Ti}^{\text{III}}$ ,  $\text{Cr}^{\text{II}}$ ,  $\text{Fe}^{\text{II}}$ ). This could explain the extreme slowness of the  $\text{Ni}^{\text{III}}$  two-phase reduction by the  $\text{Co}^{\text{II}}$  cage complex: in this case, the reducing metal center is shielded by the aliphatic part of the sarcophagine ligand and the electron transfer must occur through a much slower outer-sphere mechanism.

Another intriguing example of a two-phase redox process in which chloride ions seem to play a determining role involves aqueous iodide ion as a reducing agent. In fact, 0.1 M aqueous NaI, in the presence of 1 M NaCl, does not reduce  $[\text{Ni}^{\text{III}}\text{LCl}_2]\text{Cl}$  under two-phase conditions. This may be surprising, if one considers that  $\text{I}^-$  ( $E^0(\text{I}_2/\text{I}^-) = 0.54$  V vs NHE) is a stronger reducing agent than  $\text{Fe}^{\text{II}}$  ( $E^0(\text{Fe}^{\text{III}}/\text{Fe}^{\text{II}}) = 0.77$  V), which, in 1 M HCl, is able to reduce the nonaqueous trivalent complex. However, on addition of a  $\text{CH}_2\text{Cl}_2$  solution of  $\text{Bu}_4\text{NI}$  to a  $\text{CH}_2\text{Cl}_2$  solution of  $[\text{Ni}^{\text{III}}\text{LCl}_2]\text{Cl}$ , the reduction of the trivalent complex takes place instantaneously, and iodine forms. Moreover, reduction of the  $\text{Ni}^{\text{III}}$  complex can occur also in two-phase conditions, provided that the aqueous layer, 0.1 M NaI, is not charged with NaCl: also in this case, iodine is produced in the dichloromethane layer.

The above evidence suggests that the two-phase redox process occurs through two distinct steps: in the first step, chloride and

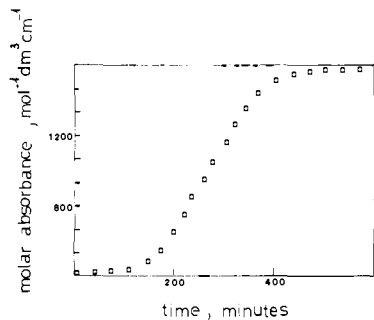


**Figure 5.** Electron transport experiments. Time dependence of the molar absorbance of the band at 340 nm of the  $\text{Fe}^{\text{III}}$  species, generated in ESP, during the  $\text{S}_2\text{O}_8^{2-}/[\text{Ni}^{\text{II}}\text{LCl}_2]/\text{Fe}^{\text{II}}$  three-phase process.

iodide ions exchange at the  $\text{CH}_2\text{Cl}_2/\text{water}$  interface and possibly an  $\text{I}^-$  ion replaces a  $\text{Cl}^-$  ion in one of the axial positions of the lipophilic complex; in the second step an intramolecular redox process occurs between the  $\text{Ni}^{\text{III}}$  center and the coordinated  $\text{I}^-$  ion. Therefore, reduction by iodide must be more correctly considered a single-phase redox process, and thus the inhibiting effect exerted by aqueous 1 M chloride is not kinetic in origin, but reflects the competition of chloride and iodide ions for extraction in the  $\text{CH}_2\text{Cl}_2$  layer.

Equation 4 indicates that an increase of the chloride concentration should push the two-phase process to the left, thus preventing the reduction of the nonaqueous  $\text{Ni}^{\text{III}}$  complex by any aqueous reducing agent. However, no chloride concentration effect has been observed in two-phase reduction of  $[\text{Ni}^{\text{III}}\text{LCl}_2]\text{Cl}$  by aqueous  $\text{Fe}^{\text{II}}$ : in particular, the rate of disappearance of the band at 324 nm does not change significantly with the HCl concentration in the aqueous layer (from 0.1 to 1.0 M). This can be ascribed to the fact that chloride ions assist the electron transfer from the metal center reducing agent: this beneficial effect probably requires only a moderate chloride concentration and should not be disturbed by an increase of the chloride concentration.

**Electron Transport Experiments.** Electron transport experiments have been designed on the basis of the experience on the two-phase redox processes described in the previous paragraphs. The experiments have been carried out using the V-shaped cell drawn in Figure 1.

The bulk liquid membrane was a  $\text{CH}_2\text{Cl}_2$  layer of 25  $\text{cm}^3$  in volume, which separated two aqueous layers, ERP and ESP, each of 25  $\text{cm}^3$ . We preferred to use a bulk liquid membrane, rather than an impregnated porous film device, in order to guarantee a greater stability of the system, even for extended periods of time. However, it will be shown that, with the presently described bulk liquid membrane cell, electron transport experiments go to completeness in a period ranging from minutes to a few hours.

In a typical experiment the membrane was  $10^{-3}$  M in  $\text{NiLCl}_2$ , the oxidizing aqueous layer, ERP, was 0.10 M in  $\text{Na}_2\text{S}_2\text{O}_8$  and 1 M in NaCl, the reducing aqueous layer was 0.01 M in one of the metal-centered reducing agents, which had been found to work in two-phase experiments, and 1.0 M in HCl.

In the transport experiments the membrane was magnetically stirred, whereas each aqueous phase was stirred by a glass rod, driven by an electric motor. Thus, hydrodynamic conditions of the present experiments are different from those experienced in the two-phase experiments previously described, where only the  $\text{CH}_2\text{Cl}_2$  layer was stirred.

Let us first consider the case in which the reducing agent is  $\text{Fe}^{\text{II}}$ . After the cell has been charged and stirring begins, the pale violet membrane takes a yellow color, due to the oxidation of  $[\text{Ni}^{\text{II}}\text{LCl}_2]$  to  $[\text{Ni}^{\text{III}}\text{LCl}_2]\text{Cl}$ . After  $\sim 1$  h, the colorless reducing aqueous layer takes a pale yellow color, whose intensity progressively increases. Appearance of the yellow color has to be ascribed to the formation of  $\text{Fe}^{\text{III}}$  species, which results from the oxidation of  $\text{Fe}^{\text{II}}$  by the  $[\text{Ni}^{\text{III}}\text{LCl}_2]\text{Cl}$  complex at the ESP/membrane interface. Portions of the ESP solution were taken at selected time intervals and their UV-vis spectra were recorded.

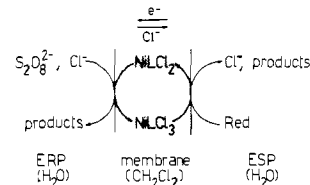


**Figure 6.** Scheme of the mechanism of the transport of electrons and countertransport of chloride ions across a liquid membrane mediated by the  $[\text{Ni}^{\text{II}}\text{LCl}_2]/[\text{Ni}^{\text{III}}\text{LCl}_2]\text{Cl}$  redox system. L, *N*-cetylcyclam.

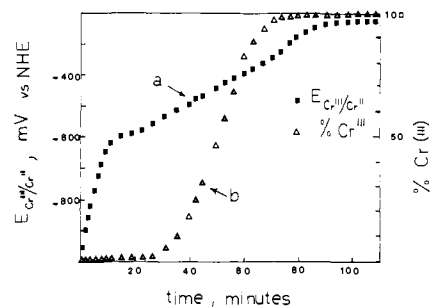


**Figure 7.** (a) Time dependence of the potential of a mercury electrode dipped in ESP during a  $\text{S}_2\text{O}_8^{2-}/[\text{Ni}^{\text{II}}\text{LCl}_2]/\text{Cr}^{\text{II}}$  three-phase experiment; the electrode potential is sensitive to the  $\text{Cr}^{\text{II}}/\text{Cr}^{\text{III}}$  redox couple; (b) plot of the %  $\text{Cr}^{\text{III}}$  in ESP vs time, calculated through the Nernst equation.

Figure 5 reports the values of the molar absorbance of the band at 340 nm, ascribed to the  $\text{Fe}^{\text{III}}$ -chloro complex, at varying times. The curve appears S-shaped and a plateau is achieved after  $\sim 500$  min.<sup>19</sup> This situation corresponds to the complete oxidation of the reducing agent in the ESP. Direct addition of solid  $\text{Na}_2\text{S}_2\text{O}_8$  did not cause any further increase of the  $\text{Fe}^{\text{III}}$  absorption band. In a blank experiment (same conditions as above, but no nickel complex in the membrane), the reducing phase remained colorless and no band developed at 340 nm.

The described three-phase oxidation and reduction diagram can be interpreted according to the scheme depicted in Figure 6, in which electrons flow from ESP to ERP and, to maintain electroneutrality in the membrane, chloride ions flow in the opposite direction.<sup>20</sup> The lipophilic tetraaza macrocyclic complex behaves as a carrier: (i) in its reduced form it carries electrons from ESP to ERP and (ii) in its oxidized form it carries chloride ions from ERP to ESP.

Cross transport of electrons and chloride ions, described by the scheme in Figure 6, was proved to occur with all the metal-centered reducing agents tested in two-phase experiments. In the case of  $\text{Cr}^{\text{II}}$ , the progress of the three-phase oxidation and reduction process could be detected visually through the color change of the aqueous reducing phase, from the pale blue of the  $\text{Cr}^{\text{II}}$  species to the blue-green of the  $\text{Cr}^{\text{III}}$  species. The  $\text{Cr}^{\text{II}}$  to  $\text{Cr}^{\text{III}}$  redox change was quantitatively monitored through the potential of a mercury electrode dipped in ESP. The potential vs time profile is reported in Figure 7 (curve a). However, the progress of the transport is probably better understood through the variation of percent concentration of  $\text{Cr}^{\text{III}}$ , calculated from the following rearranged form of the Nernst equation:

$$\% \text{Cr}^{\text{III}} = \frac{10^{(E-E^0)/0.05916}}{1 + 10^{(E-E^0)/0.05916}} \quad (5)$$

where  $E^0 = -0.43$  vs NHE. The S-shaped profile reported in Figure 7 (curve b) indicates that the electron transport is complete

(19) Absorbance corresponds to that measured at 340 nm for a solution 0.01 M of  $\text{FeCl}_3$  in 1 M HCl.

(20) Chloride ion countertransport from ERP to ESP has not been proven experimentally; it is only postulated. The small variation of the  $\text{Cl}^-$  concentration ( $10^{-2}$  M) in ESP or ERP cannot be analytically revealed in the presence of the 1 M background electrolyte (HCl or NaCl).

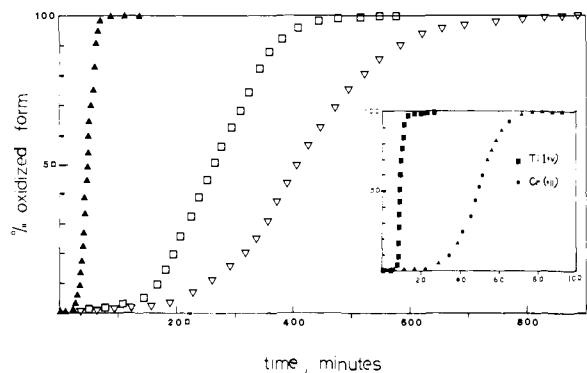


**Figure 8.** Electron transport experiments. Plot of the percent of the oxidized form of the reducing agent Red. vs time, in three-phase  $S_2O_8^{2-}/[Ni^{II}LCl_2]/Red.$  processes. Red.: ■,  $Ti^{III}$ ; ▲,  $Cr^{II}$ ; □,  $Fe^{II}$ ; ▽,  $[Co^{II}(diamsarH_2)]^{4+}$ . Concentration of the carrier in the membrane,  $10^{-3}$  M; concentration of Red. in ESP,  $10^{-2}$  M.

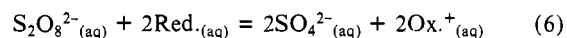
(100% of  $Cr^{III}$ ) after  $\sim 70$  min.

The fastest electron transport experiment in the present study involved  $Ti^{III}$  as reducing agent. The plot of %  $Ti^{IV}$ , calculated from the potential of a mercury electrode through the Nernst equation (5), indicates that the transport is complete in less than 15 min (see Figure 8). The end of the experiment can be visually detected through the disappearance of the violet color of the  $Ti^{III}$  species in the aqueous reducing phase. Figure 8 reports also the plot of the percent concentration of the oxidized form vs time for the most time consuming of the investigated electron transport experiments, i.e., that involving  $[Co^{II}(diamsarH_2)]^{4+}$  as a reducing agent. Perhaps, it is also the most spectacular experiment from the point of view of the color change, which parallels the electron transport: the color of the reducing aqueous phase varies from the olive green of the divalent cage complex to the bright orange color of the oxidized species. The plateau of the S-shaped profile is achieved after 700 min.

It can be observed that the rates of the electron transport experiments, qualitatively expressed by the percent variation of the concentration of the oxidized form in ESP with the time, as reported in Figure 8, follow the same sequence found for two-phase reduction tests, i.e.,  $Ti^{III} > Cr^{II} > Fe^{II} > [Co^{II}(diamsarH_2)]^{4+}$ . However, compared to two-phase tests, the three-phase device seems to discriminate much more efficiently the electron transport processes according to the nature of the reducing agent employed in ESP, experiments being complete in an impressively wide interval of time, which ranges from minutes to several hours.

## Conclusions

In the present work we have studied the redox process between aqueous peroxydisulfate and some conventional aqueous reducing agents:



However, rather than in the usual single-phase way, reaction 6 has been carried out under three-phase conditions and the oxidizing and reducing aqueous compartments have been separated by a  $CH_2Cl_2$  layer. Reaction 6 can take place in these conditions since an appropriate redox system (based on the  $Ni^{II}/Ni^{III}$  couple) ensures a cross transport of electrons and anions  $X^-$  across the bulk liquid membrane.

The process can be controlled through addition of an appropriate electrolyte  $NaX$  to the aqueous layers: when  $X = Cl$ , the reaction occurs; when  $X = ClO_4$ , the reaction does not occur. This may be considered a *thermodynamic* control, in the sense that chloride ions, through axial coordination of the metal center, stabilize the  $Ni^{III}$  oxidation state enough to permit the  $Ni^{II}/Ni^{III}$  oxidation by aqueous  $S_2O_8^{2-}$ . The much less coordinating  $ClO_4^-$  ions do not stabilize the oxidized form of the carrier enough.

Addition of  $NaCl$  to aqueous compartments may allow a further control of reaction 6. For instance, a  $Cl^-$  concentration of 1 M in the reducing aqueous phase permits reduction of the oxidized carrier by  $Fe^{II}$ , but does not allow the one by  $I^-$  (in 0.01 M concentration). Moreover, due to *kinetic* effects, oxidation of metal-centered reducing agents at the water/dichloromethane interface takes place with rates that vary dramatically with the nature of the metal. For instance, it has been shown that, with the described three-phase arrangement, oxidation of  $Cr^{II}$  in 0.01 M concentration is complete in tens of minutes and, in particular, several hours before the oxidation of equimolar  $Fe^{II}$  takes place significantly.

This type of approach to the study of redox reactions may open the way to procedures by which aqueous mixtures of reducing agents can be oxidized in a strictly selective way, through a thermodynamic and/or a kinetic control. Such a methodology appears to be relevant to selective separation of metals in solution, where variation of the oxidation state of a single cation in the mixture may strongly help its selective extraction.

**Acknowledgment.** We thank the Italian Ministry of Education (MPI 40%) for financial support.

**Registry No.** 1, 71366-36-4;  $C_{16}H_{33}Br$ , 112-82-3;  $NiCl_2$ , 118830-95-8;  $NiL(ClO_4)_2$ , 118830-96-9;  $NiLCl_3$ , 118830-97-0;  $NiL(ClO_4)_3$ , 118830-99-2; cyclam, 295-37-4;  $Ti^{3+}$ , 22541-75-9;  $Cr^{2+}$ , 22541-79-3;  $Fe^{2+}$ , 15438-31-0;  $[Co(diamsarH_2)]^{4+}$ , 85664-44-4;  $Na_2S_2O_8$ , 7775-27-1.